BIOCHEMISTRY
including biophysical chemistry & molecular biology

Article

pubs.acs.org/biochemistry

Thermodynamic Effects of the Alteration of the Axial Ligand on the Unfolding of Thermostable Cytochrome *c*

Rabindra Kumar Behera,*[,†,∥] Hiroshi Nakajima,[‡] Jitumani Rajbongshi,[†,§] Yoshihito Watanabe,[‡] and Shyamalava Mazumdar*[,†]

[†]Department of Chemical Sciences, Tata Institute of Fundamental Research, Homi Bhabha Road, Colaba, Mumbai 400005, India
[‡]Department of Chemistry, Graduate School of Science, Nagoya University, Nagoya 464-8602, Japan
[§]Department of Chemistry, Gauhati University, Guwahati 781014, India

Supporting Information

ABSTRACT: The role the axial methionine plays in the conformational properties and thermostability of the heme active site has been investigated with the help of site-specific mutations at the axial Met69 position with His (M69H) and Ala (M69A) in thermostable cytochrome c_{552} from *Thermus thermophilus*. Detailed circular dichroism, direct electrochemistry, and other spectroscopic studies have been employed to investigate the thermally induced and GdnHCl-induced unfolding properties of the heme active site of the wild type and the mutants of cytochrome c_{552}. We observed an unusually high thermodynamic and thermal stability of the M69A mutant compared to that of wild-type cytochrome c_{552}. However, the M69H mutant exhibited a slightly lower unfolding free energy compared to that of the wild-type protein. The high conformational stability of the M69A mutant was attributed to the presence of residual structure in the unfolded state as well as to the altered conformation in the folded state of this mutant of cytochrome c_{552}. This study thus supports the view that apart from the folded state, the unfolded state of a protein may also make a significant contribution to the stability of a protein.

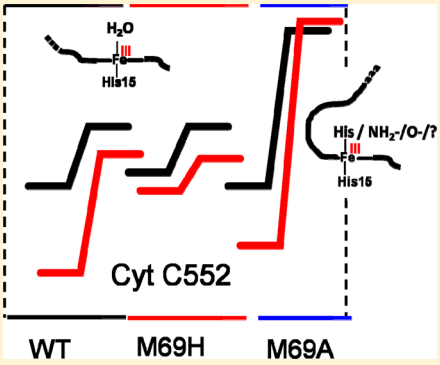

The heme proteins play a variety of roles in biological systems, including electron transport, oxygen storage and delivery, catalysis, etc.[1,2] This diverse nature of their mode of action has been attributed either to the differences in their axial ligands or to the differences in the amino acid residues around the heme active site.[3] In addition, the axial ligands and the surrounding residues in the heme proteins have also been shown to play crucial roles in conformational stability.[4−12] Earlier studies showed that the removal of the axial ligands from horse cytochrome *c*, myoglobin, and cytochrome b_{562} alters the folding and decreases the conformational stabilities of the proteins.[4−7] A detailed assessment of the specific effects of the amino acid axially coordinated to the iron of the heme on the conformational stability is, however, often limited because of the low thermal stability of the protein. The study of the conformational stability of a hemeprotein from a thermophilic source would hence immensely help in the understanding of the role of the axial ligands in the thermodynamic properties of the active site of the protein. Several thermophilic proteins have recently been investigated from both experimental and theoretical perspectives to gain insight into the molecular basis of protein thermostability.[13−19] Structural comparison between the thermophilic proteins and their mesophilic homologues has contributed significantly to the understanding of the relationship between protein structure and thermostability. The presence of large networks of ion pairs,[17,19] hydrogen bonds or an increased packing density,[20] a hydrophobic core,[21] etc., has been found to be responsible for the thermostability of the thermophilic proteins. The metalloproteins can indeed show further stabilizing interactions through metal−ligand (from protein) coordination.

The release of the prosthetic group during unfolding or other types of conformational changes can complicate the studies of stability of the heme proteins.[4,5] A six-coordinate *c*-type heme protein such as cytochrome *c* and analogues that consist of the heme moiety covalently attached to the protein matrix through thioether linkages with two cysteine residues offer a preferred system for studying the role of axial coordination in the conformational stability of the heme protein. Although cytochrome *c* has previously been engineered (axial methionine to alanine) to create an artificial globin and peroxidase, the effects of such mutations on the conformational stability have not been reported.[8,22,23]

Cytochrome c_{552} (cyt c_{552}) is a thermostable *c*-type heme protein from *Thermus thermophilus* (HB8) involved in the terminal step of the bacterial respiratory electron transfer process.[24] The active site of cyt c_{552} [Protein Data Bank (PDB) entry 1C52] consists of a low-spin iron(III) in a ruffled shaped heme group axially coordinated to His15 and Met69 (Figure 1).

Received: July 22, 2012
Revised: January 19, 2013
Published: January 22, 2013

dx.doi.org/10.1021/bi300982v | *Biochemistry* 2013, 52, 1373−1384

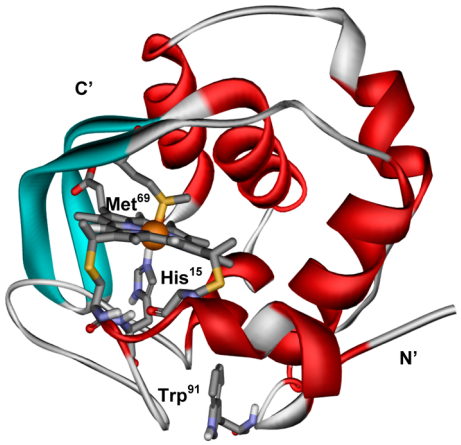

Figure 1. Crystal structure (PDB entry 1C52) of thermostable cytochrome c_{552} from *T. thermophilus* illustrating the heme group, axial ligands (His15 and Met69), the Trp91 residue, and the N-terminal and C-terminal helices.

The crystal structure of cyt c_{552} shows the presence of a covalently bound heme with thioether linkages to two cysteine residues in a conserved Cys^{11}-Xaa^{12}-Yaa^{13}–Cys^{14}-His^{15} motif.[25] The second axial ligand, Met69, is present at the end of an unusual extended β-sheet (Leu^{54}–Met^{69}) covering one edge of the heme (Figure 1). Residues such as V49, L50, L54, Q55, V68, M69, and F72 form a compact hydrophobic environment around the distal heme pocket, which has been proposed[25] to be important for the high thermostability of this protein (Figure S1 of the Supporting Information).

We have investigated the effect of axial coordination on the thermodynamic and thermal stability as well as the on the redox properties of cyt c_{552}. Site-specific mutation of the axial Met69 to a His or an Ala was conducted to create M69H and M69A mutants of cyt c_{552}. Direct electrochemical studies, circular dichroism studies, and other spectroscopic studies have been conducted to determine the thermally and chemically induced unfolding properties of the M69H and the M69A mutants in comparison with those of the wild-type (WT) protein. The results are discussed in light of our understanding of the molecular basis of the role of axial ligation in the stability and function of the hemeprotein.

MATERIALS AND METHODS

Materials. Carboxy methyl (CM) Sepharose and Sephadex G-25 columns were purchased from GE Healthcare Bio-Sciences AB (Uppsala, Sweden). Guanidine hydrochloride (GdnHCl), ampicillin sodium salt, isopropyl β-D-thiogalactopyranoside (IPTG), lysozyme, phenylmethanesulfonyl fluoride (PMSF), and DNase I were purchased from Sigma Chemical Co. All buffer components, solvents, and other reagents were of analytical grade. Deionized water (Millipore) was used in the preparation of all the buffers.

Mutation, Expression, and Purification of Recombinant cyt c_{552}. Site-directed mutagenesis was conducted using the QuikChange mutagenesis kit (Stratagene Co.). The forward and reverse oligonucleotide primers used for the M69H mutation were 5′-GAAGTACAACGGCGTCCACTCCTCC-TTCG-3′ and 3′-CTTCATGTTGCCGCAGGTGAGGAGG-AAGC-5′, respectively. The forward and reverse oligonucleotide primers used for the M69A mutation were 5′-GAAGTA-CAACGGCGTCGCGTCCTCCTTCG-3′ and 3′-CTTCATGTTGCCGCAGCGCAGGAGGAAGC-5′, respectively. The underlined nucleotide sequences are those corresponding to the amino acid residues of mutagenesis. WT cyt c_{552} and mutant proteins were expressed using *Escherichia coli* (strain JM109-DE3) cells transformed with the pET-22b(+)-c552 plasmid and cyt *c* maturation gene (pACYC-CCMO) and purified according to a reported method.[23] The cell pellets were lysed (by ultrasonication) and centrifuged to remove cell debris and membranes. The supernatant was incubated at 70 °C for 30 min and centrifuged to remove any denatured mesophilic proteins. The supernatant was loaded onto a pre-equilibrated CM Sepharose column with 50 mM sodium succinate buffer (pH 5.0), and the proteins were eluted by applying a linear gradient from 0 to 1 M NaCl. The protein fractions having R_z (A_{Soret}/A_{280}) values of ≥5, 4, and 6.5 for WT, M69H, and M69A proteins, respectively, were collected and finally desalted with a Sephadex G-25 column equilibrated with 50 mM sodium phosphate buffer (pH 7.0). The concentrations of the WT and mutant cyt c_{552} proteins were determined by the pyridine–hemochrome method.[26]

Spectroscopy. The WT and mutant cyt c_{552} proteins in 50 mM sodium phosphate buffer (pH 7.0) were used for recording UV–visible absorption spectra on a Shimadzu (UV-2100) spectrophotometer coupled with a thermostated cell holder (TCC-260 temperature controller). The concentration of the protein was 4 μM for recording UV–visible absorption spectra. CD spectra were recorded on a JASCO J-810 spectropolarimeter equipped with a Peltier cell temperature controller (±0.2 °C). The far-UV CD spectra (195–250 nm) were recorded using a quartz cuvette with a 1 mm path length. The near-UV and visible CD (heme CD) spectra (250–450 nm) were recorded using a cuvette with a 1 cm path length. The concentration of the protein samples was 16 μM for recording both far-UV and visible CD spectra for WT and mutant cyt c_{552} proteins. The far-UV CD spectra were fit to Reed's algorithm (received with CD instruments) to estimate the secondary structure for all the species.

Thermal and Chemical Unfolding Study. The temperature dependence of the far-UV CD (at 222 nm) and the heme CD (at 404, 402, and 398 nm for WT, M69H, and M69A proteins, respectively) were monitored to determine the thermal unfolding of the secondary and tertiary structure around heme of WT and mutant cyt c_{552} in 50 mM sodium phosphate buffer (pH 7.0) at different GdnHCl concentrations. Cuvettes with 1 and 10 mm path lengths were used for far-UV and heme CD, respectively. The temperature was increased from 5 to 90 °C at a heating rate of 1 °C/min. Protein samples (16 μM) were used both for the far-UV and the heme CD studies. The protein solutions were equilibrated with various GdnHCl concentrations (0–7 M) at 4 °C for 36 h for the unfolding studies. The GdnHCl concentration in the stock solution was determined using a refractometer according to the reported methods.[27]

The unfolding studies with the WT and mutant cyt c_{552} proteins with GdnHCl as the denaturant were also performed by monitoring the Soret absorbance peaks as a function of GdnHCl concentration at 25 °C. The protein samples [4 μM, in 50 mM sodium phosphate buffer (pH 7.0)] were incubated under the same condition described above prior to the scanning of UV–visible absorption spectra.

Analysis of the Unfolding Data. The results were analyzed by a two-state equilibrium between the folded state (N) and the unfolded state (U):

dx.doi.org/10.1021/bi300982v | *Biochemistry* 2013, 52, 1373–1384

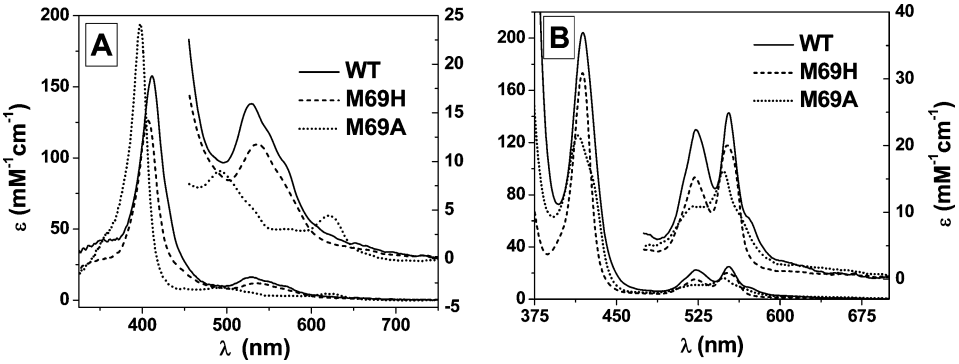

Figure 2. (A and B) UV−visible absorption spectra of the native forms of ferric (A) and ferrous (B) WT (—), M69H (---), and M69A (···) cyt c_{552} in 50 mM sodium phosphate (pH 7.0) at 25 °C.

$$N \rightleftharpoons U$$

The free energy change of unfolding (ΔG_U) is defined as

$$\Delta G_U = -RT \ln K_U = -RT \ln\left(\frac{f_U}{1 - f_U}\right) \quad (1)$$

where R is the gas constant, K_U is the equilibrium constant for unfolding, and f_U is the fraction of the total protein in the unfolded conformation. f_U is obtained by

$$f_U = \frac{y_0 - (y_N + m_N x)}{y_U + m_U x - (y_N + m_N x)} \quad (2)$$

where y_0 is the observed CD values (millidegrees) of the WT and mutant cyt c_{552} at a given temperature (or at a given GdnHCl concentration), y_N and y_U represent the intercepts, x is GdnHCl concentration, and m_N and m_U are the slopes of the native and unfolded baselines, respectively.

The unfolding curves of the proteins induced by denaturants at different temperatures were analyzed from the linear dependence of ΔG_U on denaturant concentration as

$$\Delta G_U = \Delta G^{Aq} - m[\text{GdnHCl}] \quad (3)$$

where ΔG^{Aq} and [GdnHCl] are the free energy extrapolated to zero concentration (LEM) of GdnHCl and the concentration of GdnHCl, respectively. Linear fits to the transition region of the experimental unfolding data (ΔG_U) give m values and the free energies of unfolding in aqueous solution, ΔG^{Aq}, at different temperatures.[28,29]

The data were also analyzed by a nonlinear fit to eq 3a by combining eqs 1−3:

$$y_0 = \left[y_N + m_N x - (y_U + m_U x) \times e^{(\Delta G^{Aq} - mx)/RT}\right] \Big/ \left[1 - e^{(\Delta G^{Aq} - mx)/RT}\right] \quad (3a)$$

The stability curves for WT and mutant cyt c_{552} were obtained for secondary and tertiary structure around heme by nonlinear square analysis of the data given above (ΔG^{Aq} as a function of temperature) by fitting to the Gibbs−Helmholtz equation.

$$\Delta G_T^{Aq} = \Delta H_m(1 - T/T_m) + \Delta C_p[T - T_m - T \ln(T/T_m)] \quad (4)$$

Different thermodynamic parameters such as ΔH_m, T_m, and ΔC_p for unfolding of the secondary and tertiary structures around the heme were obtained from the analyses of the respective stability curves of WT and mutant cyt c_{552} proteins. The results are reported with the standard errors obtained from the fit of the data. The total error of determination of the parameters would, however, include the uncertainties in measurements and propagate errors, which are estimated to be within 15% of the reported values.

Electrochemistry. Direct measurement of the reduction potential of cyt c_{552} and its mutants was conducted using Autolab potentiostat 30 (Eco-Chemie) operated using GPES. The lab-made electrochemical cell consisted of a three-electrode system: a glassy carbon (GC) working electrode (which was in direct contact with 50 μL of a protein-containing solution), a platinum counter electrode, and a Ag/AgCl (3 M KCl) reference electrode. The GC and Ag/AgCl (3 M KCl) electrodes were from CH Instruments. Potassium phosphate buffer (50 mM, pH 7.0) along with 0.1 M KCl was used as the supporting electrolyte. Cyclic voltammetric measurements were taken at scan rates of typically 5 mV/s, and square wave voltammetric measurements were taken a frequency of 8 Hz at 25 °C. A nitrogen atmosphere was maintained over the solutions during the experiments. All reduction potentials were with reference to the NHE.

Samples were prepared by equilibrating the protein solution (0.5 mM, stock concentration) with different concentrations of guanidinium hydrochloride for 36 h at room temperature followed by concentration by using Millipore ultra centricon tubes. Prior to every experiment, suitable pretreatment of the working electrode was conducted. Pretreatment of the GC electrode involved polishing firmly on micro-cloth using fine 0.05 μM alumina powders. It was then sonicated for 2−3 min in Milli-Q water, rinsed thoroughly with Milli-Q water, dried under nitrogen for 5 min, and then used immediately.

RESULTS AND DISCUSSION

UV−Visible Absorption Study. The UV−visible absorption spectra of WT, M69H, and M69A cyt c_{552} in their ferric and ferrous states are shown in panels A and B of Figure 2, respectively. The peak positions corresponding to Soret (γ) and visible regions (α and β) of the WT and mutant proteins are listed in Table ST1 of the Supporting Information. The absorption spectral features of WT cyt c_{552} agree with those from an earlier report that are characteristic of class I c-type cytochromes and correspond to the low-spin His-heme-Met axial coordination.[30] The ferric form of the M69H mutant showed an ∼3 nm blue-shifted Soret band compared to that of WT cyt c_{552}. The ferric and ferrous forms of M69A mutant cyt c_{552} show drastically different spectral features compared to

dx.doi.org/10.1021/bi300982v | Biochemistry 2013, 52, 1373−1384

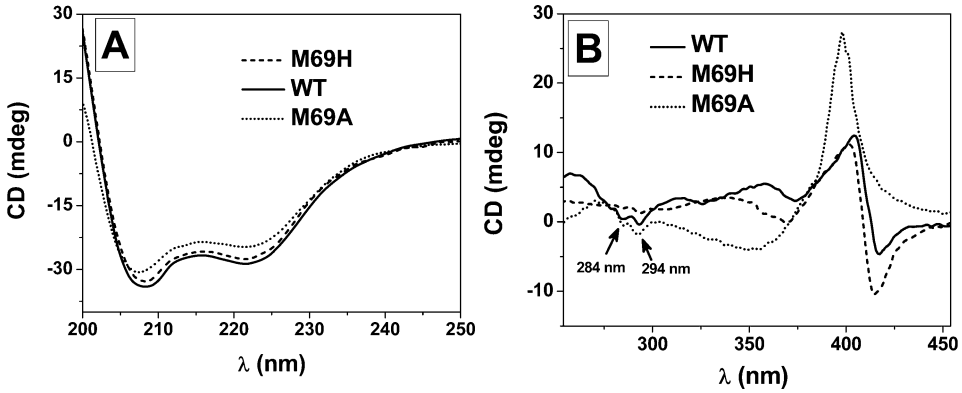

Figure 3. (A and B) Far-UV CD spectra (A) and near-UV and heme CD spectra (B) of ferric WT (—), M69H (---), and M69A (···) cyt c_{552} in 50 mM sodium phosphate buffer (pH 7.0) at 25 °C. The concentrations of all variants of cyt c_{552} were 16 μM. The path length of the cuvette for far-UV CD studies was 1 mm, and that for near-UV and heme CD was 10 mm.

those of the WT and M69H mutant proteins. The ferric form of the M69A mutant showed a blue-shifted Soret band at 398 nm, a broad peak at 493 nm, and a shoulder at 538 nm in addition to a new small absorption band at 625 nm. This new band at 625 nm of the M69A mutant is similar to that found in the HRP, met-myoglobin, several mutants of these heme proteins, and the substrate-bound cytochrome P450. This band has been assigned as a characteristic charge transfer (porphyrin-to-iron pπ−dπ charge transfer) band in the high-spin ferric heme system (see Table ST1 of the Supporting Information).[31−34] These results indicate that while the ferric forms of M69H and WT cyt c_{552} are low-spin six-coordinate species, the replacement of the axial methionine ligand with alanine leads to formation of a high-spin ferric species. These observations about the low-spin (WT) and high-spin (M69A) nature of the ferric heme iron were also well supported by ^{1}H NMR spectra (Figure S2 of the Supporting Information) of WT and M69A mutant cyt c_{552}. The heme methyl ^{1}H chemical shift of WT cyt c_{552} was found to show low-spin spectral characteristics at ∼34 and ∼32 ppm in the downfield region, which are similar to those of WT cyt *c* from horse heart,[35] but the heme methyl ^{1}H signals of the M69A mutant are found to be shifted even more toward the downfield region around 60−70 ppm. The highly downfield chemical shifts were characteristic of the high-spin Fe(III) nature of the M69A mutant.[36−38] The NMR spectra further show that the meso-protons are not upfield-shifted in the M69A mutant, indicating that the heme is possibly six-coordinate in the M69A mutant of cyt c_{552}.[37,38]

Circular Dichroism and Fluorescence Studies. The CD spectrum in the far-UV region provides information about the nature and composition of different secondary structural elements such as α-helices, β-sheets, turns, and random coils[39] in a protein. The far-UV CD spectra for WT, M69H, and M69A cyt c_{552} are shown in Figure 3A. The presence of two negative bands at 208 and 222 nm in the far-UV CD spectra of WT, M69H, and M69A cyt c_{552} supports the proposal that the α-helices are the major secondary structural elements present in both WT and mutant cyt c_{552}. Close inspection of the results in Figure 3A shows that though the mutation of the axial methionine to histidine in the M69H mutant has no effect on the far-UV CD spectrum of cyt c_{552}, the band near 208 nm for the M69A mutant was slightly blue-shifted from the corresponding band of WT c_{552}. The far-UV CD spectra were analyzed using Reed's algorithm,[40] which suggests a small increase in the level of random coil in the M69A mutant compared to that in WT cyt c_{552} at the expense of α-helices and turns (see Table ST2 of the Supporting Information).

The near-UV and visible CD (heme CD) spectra for WT, M69H, and M69A cyt c_{552} are shown in Figure 3B. The two CD bands at 284 and 293 nm in the near-UV region are the signatures of the asymmetric environment around the tryptophan residues in cyt c_{552}.[39] Figure 3B clearly shows that the tryptophan tertiary environment has been affected because of the axial ligand mutation in thermophilic cyt c_{552}.

The steady state intrinsic (Trp91) fluorescence spectra of the WT protein showed very a low quantum yield, while mutation of the axial methionine to histidine or alanine showed significant enhancement of the fluorescence emission (Figure S3 of the Supporting Information). The emission of the single tryptophan (Trp91) of the protein is quenched by the transfer of resonance energy to the heme that is located ∼8.5 Å from the fluorophore in the WT protein. The enhancement of fluorescence in the M69H and M69A mutants suggests that the segment that follows the Met69 residue in the protein possibly moves away from the heme in the mutants, supporting the change in the tertiary structure of the protein upon mutation of the axial ligand.

The circular dichroism of the heme absorption arises because of the anisotropic interaction of the heme chromophore with the nearby aromatic residues in the protein. The heme CD thus contains information about the relative spatial arrangements of the heme and the aromatic side chains in the tertiary structure of the protein.[41] The heme CD spectrum of WT cyt c_{552} exhibits a strong positive band at ∼404 nm and a negative band at 417 nm (Figure 3B), which agrees well with the previous report.[24] The heme CD spectrum (Figure 3B) of M69H cyt c_{552} shows symmetrical positive (at 402 nm) and negative (at 414 nm) bands. The M69A mutant, on the other hand, shows an intense positive band (at 398 nm) in the Soret region and a broad negative band in the delta region (Figure 3B). The changes in the axial ligation and/or conformational properties of the heme cavity may affect the position and nature of the heme CD bands of the protein.[41,42] The small blue shift in the position(s) of the heme CD bands (Figure 3B) in the mutants may be related to the blue shift in the Soret absorption bands (Figure 2A) caused by changes in the coordination geometry of the metal ion in the mutants. The absence of a negative CD band (at ∼417 nm) in the heme tertiary region of the M69A mutant may be ascribed to the changes around the heme center

dx.doi.org/10.1021/bi300982v | *Biochemistry* 2013, 52, 1373−1384

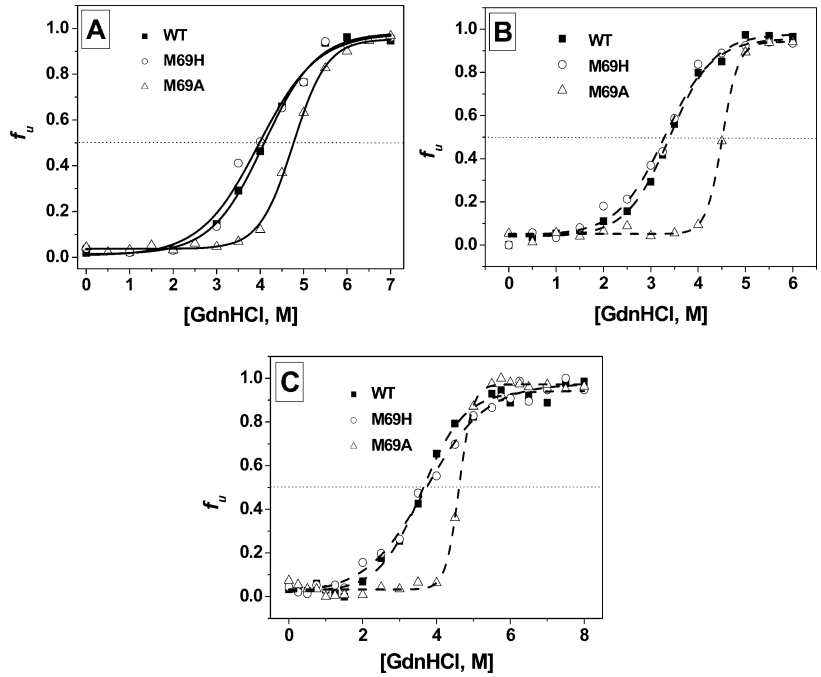

Figure 4. (A–C) GdnHCl-induced unfolding profiles for the secondary structure (A), heme tertiary structure (B), and UV–visible absorption (C) of ferric WT (■), M69H mutant (○), and M69A (△) mutant cyt c_{552} at 25 °C in 50 mM sodium phosphate (pH 7.0). Solid lines through the data in panel A correspond to fits to eq 3a. The dashed lines in panels B and C are sigmoidal fits to the data. The unfolding of the secondary structure was monitored by the CD band at 222 nm. However, the unfolding of the heme tertiary structures was monitored at their respective Soret CD and Soret UV–visible absorption bands.

caused by the absence of the axial methionine residue in the mutant protein.

Thermally Induced and GdnHCl-Induced Unfolding. To determine whether axial coordination in the protein plays any role in the stability of the active site, we conducted detailed thermodynamic stability studies of the wild type and mutants of cyt c_{552}. It is important to note that addition of GdnHCl to the protein solution leads to equilibrium unfolding of the secondary as well as tertiary structure of the protein. Unfolding of cyt c_{552} was reversible as observed from the reversal of the CD signal as well as from the color of the protein solution. It is noteworthy that the M69A mutant reversibly changes color from light blackish green to red during folding and unfolding. However, an increase in temperature alone was insufficient to completely unfold WT and mutant proteins because of the thermostability of cyt c_{552}. The temperature-dependent circular dichroism studies show that WT and the mutants of cyt c_{552} do not unfold completely even at 90 °C in the absence of GdnHCl. Thus, the unfolding of WT and mutant cyt c_{552} with GdnHCl was studied at different temperatures to assess the effect of the mutation of the axial ligand on the conformational stabilities by monitoring the CD signals both in the far-UV region (Figure 4A) and in the heme tertiary region (Figure 4B) as well as by monitoring the absorbance of the Soret band of the WT and mutant protein (Figure 4C) at 25 °C.

The GdnHCl-induced unfolding profiles of oxidized WT and mutant cyt c_{552} could be analyzed by a two-state model. Earlier reports also suggested that the unfolding of cyt c_{552} from *T. thermophilus* proceeds by a two-step process (see below).[43,44] Analyses of the unfolding data were performed by using eqs 1–4 of Materials and Methods. The unfolding transition profiles clearly suggest that the M69A mutant unfolds at a higher GdnHCl concentration than WT and M69H mutant cyt c_{552} (Figure 4). The C_m value (midpoint of the unfolding transition, $[GdnHCl]_{1/2}$) obtained from the analysis of far-UV CD for the M69A mutant (4.7 ± 0.1 M at 25 °C) was found to be higher than those of both WT (4.1 ± 0.1 M at 25 °C) and M69H (4.0 ± 0.1 M at 25 °C) cyt c_{552}. The C_m value of WT cyt c_{552} obtained from the secondary structure unfolding analysis matches with that reported previously (4.2 ± 0.2 M).[43] The C_m value obtained from the analyses of the heme CD spectra (probing the tertiary structure around the heme) for the M69A mutant (4.5 ± 0.1 M at 25 °C) was found to be higher than those of both WT (3.4 ± 0.1 M at 25 °C) and M69H (3.3 ± 0.1 M at 25 °C) cyt c_{552}. The C_m value obtained from the analysis of the absorbance of the Soret band of the M69A (4.2 ± 0.2 M) mutant was also higher than those of WT (3.6 ± 0.2 M) and M69H (3.7 ± 0.2 M) cyt c_{552}. It is important to note that though the unfolding profiles of the protein could be analyzed using a simple two-state model, the values of the midpoint (C_m) were distinctly different for the far-UV CD and for the heme CD. This indicates that the unfolding process in this case possibly involves multiple states and the different spectroscopic experiments could probe different states, leading to the observation of the apparent two-state transitions.

The apparent free energies of unfolding in aqueous solution, ΔG^{Aq}, were obtained for WT and mutant cyt c_{552} by the linear extrapolation method (eq 3) from the denaturant-dependent changes in the far-UV CD at each temperature (Figure 4A). The results (Table 1) show that the ΔG^{Aq} for unfolding decreased upon mutation of the M69 residue to His (in the M69H mutant). On the other hand, mutation of this residue to Ala (in the M69A mutant) led to a distinct increase in the ΔG^{Aq} for unfolding of the secondary structure of the protein (Table 1) at room temperature (see below). The spectral changes of the heme (absorbance as well as CD) at different denaturant concentrations (Figure 4 B,C) were complicated because of contributions from several factors apart from the structural

dx.doi.org/10.1021/bi300982v | *Biochemistry* 2013, 52, 1373–1384

Table 1. Summary of Thermodynamic Parameters for the Secondary Structure (from far-UV CD) of Oxidized Forms of WT, M69H, and M69A cyt c_{552} from *T. thermophilus*[a]

protein	ΔG^{Aq} (kJ/mol) [m (kJ/mol^2)]	T_m (K)	ΔC_p (kJ mol^{-1} K^{-1})	ΔH_m (kJ mol^{-1})
WT	13 ± 2 [3.1]	368 ± 3	1.3 ± 0.2	127 ± 2
M69H	10 ± 2 [2.7]	366 ± 2	1.2 ± 0.2	118 ± 1
M69A	34 ± 2 [7.3]	372 ± 2	2.1 ± 0.2	248 ± 2

[a] ΔG^{Aq} and m were determined at 298 K, and T_m, ΔH_m, and ΔC_p were determined from nonlinear curve fitting of the respective protein stability curves to the Gibbs–Helmholtz equation.

changes. Moreover, the heme CD and the absorbance of the M69A mutant of cyt c_{552} (Figure 4B,C) were further complicated because of the presence of residual structure in the unfolded protein (Figure 5). Hence, the denaturant-dependent changes in the heme CD as well as in the absorption spectra (Figure 4B,C) of the protein were not analyzed to derive any thermodynamic parameters.

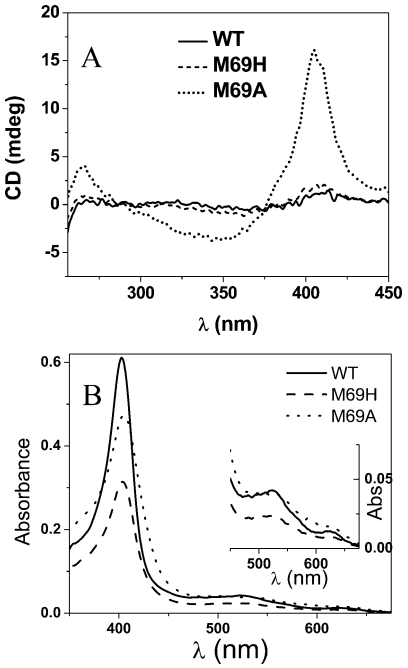

Figure 5. (A) Heme CD spectra and (B) UV–visible absorption spectra of unfolded ferric WT (—), M69H mutant (---), and M69A mutant (···) cyt c_{552} in 7 M GdnHCl (pH 7.0) at 90 °C. The concentrations of all variants of cyt c_{552} were 16 μM for the heme CD and 4 μM for UV–visible absorption studies.

Circular Dichroism Spectra under Different Unfolding Conditions. As discussed in the previous section, the proteins were not completely unfolded in aqueous buffer solutions even at 90 °C, and unfolding of the proteins could be studied at high temperatures in the presence of GdnHCl. The heme CD spectral profiles during unfolding of WT cyt c_{552} (spectra not shown) and the M69H mutant were found to be similar. Both the positive and negative heme CD bands of WT and M69H (Figure S4A of the Supporting Information) were decreased in magnitude upon unfolding, leading finally to almost no Cotton effect (CD activity) of the heme band in the unfolded protein (Figure 5). Earlier studies of unfolding of horse heart cyt c, however, reported an increase in the magnitude of the positive band of the heme CD at the expense of the negative CD band[41,45−47] because of the formation of a misfolded species. The absence of a heme CD band in the unfolded form of WT and M69H cyt c_{552} in this case indicates that the anisotropic environment around the heme is possibly absent in the unfolded form of the protein.[41,46] These results support the earlier report that unlike horse cyt c, unfolding of WT cyt c_{552} follows the "on pathway" and possibly does not involve formation of any misfolded heme species.[44,48]

The heme CD spectral profiles during unfolding of the M69A (Figure S4B of the Supporting Information) mutant were found to be different from those of both WT and M69H mutant cyt c_{552}. A new positive CD band at 407 nm emerged via the loss of the original positive CD band intensities at 398 nm of the M69A mutant upon unfolding (Figure S4B of the Supporting Information). The results described above indicate that the unfolding pathway for the M69A mutant is different from that of both WT and M69H mutant cyt c_{552}.

Figure 5A shows the heme CD spectra of ferric WT, M69H, and M69A cyt c_{552} in the presence of 7 M GdnHCl (pH 7.0) at 90 °C. The results indicate that the tertiary structures around the heme center of WT and M69H cyt c_{552} are possibly completely unfolded [i.e., the environment around the heme is isotropic in the unfolded form (Figure 5)] at 90 °C in the presence of 7 M GdnHCl. On the other hand, the heme environment remains anisotropic in the case of unfolded M69A cyt c_{552} at 90 °C in the presence of 7 M GdnHCl (Figure 5), suggesting the existence of residual structure. The possibility of formation of complex structures (e.g., misfolded or oligomeric forms) of the M69A mutant with the heme center trapped in an anisotropic environment cannot be ruled out under denaturing conditions, and such complex structures may lead to the observation of residual structure around the heme in the M69A mutant of cyt c_{552}.

UV–Visible Absorption Spectra under Different Unfolding Conditions. Unfolding of WT cyt c_{552} and its mutants at increasing GdnHCl concentrations showed a gradual decrease in the absorbance of the Soret band (see Figure S5A of the Supporting Information). The unfolding (in 7 M GdnHCl) caused shifts in the Soret band position from 410 to 403 nm in the WT protein, from 407 to ∼403 nm in the M69H mutant, and from 398 to ∼407 nm in the M69A mutant (Figure 5 and Figure S5 of the Supporting Information). Both the WT and M69H mutant showed the presence of a distinct band at ∼632 nm indicating the presence of a high-spin heme species in the unfolded protein. Unfolding of the M69A mutant, however, caused a decrease in the absorbance of the 625 nm band, indicating a decrease in the high-spin species, though even at 7 M GdnHCl there was a very weak band at ∼630 nm, indicating the possible presence of a mixture of low-spin (major) and high-spin (minor) forms.

The thermal unfolding of the WT and the mutants of the protein also showed qualitatively similar trends in the absorption spectra as observed in the case of GdnHCl-induced unfolding, indicating that the thermally induced and GdnHCl-induced unfolding processes might form similar species (see Figures S4 and S5 of the Supporting Information). The thermal unfolding of the M69A mutant consisting of a high-spin ferric heme in the folded form showed a clear isosbestic point possibly associated with ligand exchange at high temperatures in the presence of GdnHCl. These results suggest that the M69A mutant possibly has a heme ligand coordination different compared to that of the WT and M69H mutant of cyt c_{552} in

the unfolded state at a high GdnHCl concentration and 90 °C. It is important to note that the absorption spectrum of the unfolded M69A mutant (in 7 M GdnHCl) showed a distinct shift in the Soret band from ∼407 nm at pH 7 (Table ST1) to 402 nm (data not shown) with an increase in absorbance at 630 nm at pH 4, indicating formation of a high-spin heme species of the unfolded M69A mutant of cyt c_{552} at low pH.

Earlier reports have shown that both the thermodynamic stability and the thermal stability of cyt *c* are sensitive to the protein environment around the heme.[49−51] It has also been proposed previously that fluxionality of the axial methionine in the folded state is critical for the high thermal and thermodynamic stability of thermophilic cyt c_{552} from *Hydrogenobacter thermophilus* (*Ht* cyt c_{552}).[49−52] These results suggest that the M69A mutant confers an unusually increased conformational stability to the heme pocket compared to that of WT cyt c_{552}. Site-directed mutagenesis of Met61 to His in *Pseudomonas* cyt c_{551} was previously shown to decrease the stability compared to that of the WT protein.[53] Earlier reports also showed that the stability of the tetraheme cyt c_3 from *Desulfovibrio vulgaris*[54] with an active site containing a His/His coordination to the heme was increased by converting the His/His system to a His/Met coordination to the heme, which supports our results for the M69H mutant of cyt c_{552}.

The heme CD spectra of both WT and M69H cyt c_{552} in the unfolded state are similar to that reported for acid-unfolded horse heart cyt *c* at pH 2.5, which was proposed to have a His/H_2O axially coordinated heme species.[46] Thus, unfolding of the protein possibly leads to removal of the axial Met (in WT) or (distal) His (in M69H) coordination of the protein. The heme CD spectrum of unfolded M69A cyt c_{552}, on the other hand, was similar to that reported for the unfolded (misfolded) horse heart cyt *c* at neutral pH. The Soret band position of the unfolded M69A mutant [∼407 nm (Figure 5)] was also similar to that of folded M69H (Table ST1 of the Supporting Information), possibly indicating the presence of a six-coordinate low-spin heme in a misfolded conformation. However, earlier studies of the M80A mutant of yeast iso-1-cytochrome *c* proposed the formation of a hydroxyl-ligated ferric heme[55] upon unfolding, which showed a Soret band at 406 nm. Thus, unfolding of the M69A mutant of cyt c_{552} might also lead to formation of a hydroxyl-ligated ferric heme (i.e., OH or Tyr coordinated to heme) in a misfolded conformation.[46,56−58] The position of the UV−visible absorption band depends on the coordination geometry, the spin state, the nature of the axial ligands, and the environment around the heme center, and unambiguous assignment of the axial coordination of the heme in the unfolded M69A mutant of cyt c_{552} could not be made on the basis of our results.

The *m* values for unfolding determined from the analyses of the far-UV CD results of the proteins in the oxidized state are listed in Table 1. The high *m* for the M69A mutant indicates an apparently expanded structure of the unfolded protein compared to those of the WT and M69H mutant in the oxidized forms. The heme CD and electrochemical studies, however, indicated that the unfolded form of the M69A mutant might have a residual structure near the heme. This possibly indicates that the distal loop containing the M69 residue might be more open to allow formation of a misligated heme with a certain residue away from the M69 site.

Comparison of the sequences of cyt *c* from horse heart (PDB entry 1HRC) and yeast (PDB entry 1YCC) and cyt c_{552} (*Ht* cyt c_{552}) from *H. thermophilus* (PDB entry 1YNR) with the sequence of cyt c_{552} from *T. thermophilus* (1C52) shows (Figure S8 of the Supporting Information) that the two Cys residues and the coordinated His are invariant in all four proteins. While the axial Met residues in horse and yeast cytochromes are homologous, Met59 of cyt c_{552} from *H. thermophilus* and Met69 of cyt c_{552} from *T. thermophilus* do not have any homologous residue in the other proteins. Unfolding of the protein would break the iron−Met bond, leading to the movement of the protein segment at the distal side of the heme. Misfolded structures with coordination of His33 and less commonly His26 as the non-native ligands in horse cyt *c* were reported previously.[58] Cyt c_{552} does not contain any His residue homologous to His33 or His26 of horse cyt *c*; hence, the misfolded structures analogous to that of horse cyt *c* are not formed in the case of WT cyt c_{552}. Mutation of Met69 to Ala (in the M69A mutant of cyt c_{552}) possibly results in a higher flexibility and more open conformation of the distal segment of the mutant protein. Misfolding of the unfolded M69A mutant may hence result from coordination of a non-native residue (e.g., His86, Gln74, Lys101, etc.) from the distal side of the heme or from coordination of a residue from another molecule of the protein forming a domain-swapped soluble dimer. Similar domain-swapped dimers were recently shown in an ethanolic solution of *H. thermophilus* cyt c_{552} and horse cyt *c*.[59,60] Although the distal region of the heme in the M69A mutant of cyt c_{552} may be relatively more flexible than that in the WT or in the M69H mutant of the protein, the exact structural basis for formation of the residual structure upon unfolding of the M69A mutant could not be identified in this study.

Stability Curves of the Proteins. The thermodynamic stability (free energy of unfolding) of a protein is defined as the difference between the free energies of the native and unfolded states ($\Delta G_{Unf} = G_U - G_F$). The free energies of the folded and unfolded states of a protein arise from the different types of interactions (intraprotein and solvent−protein) present in their respective states. Hence, both the folded and unfolded state structures contribute to the overall thermodynamic stability of the proteins. Protein stability has often been described only on the basis of the properties of the folded state of the protein. However, recent studies show distinct evidence that suggests that residual structures in the unfolded state contribute substantially to the thermodynamic stability of the protein in its folded form.[35,61−63]

The plot of the conformational stability (ΔG^{Aq}) of the protein versus temperature is known as the "protein stability curve" defined by the modified Gibbs−Helmholtz equation (eq 4).[28,64] The nature of the stability curve depends on how different thermodynamic parameters such as ΔH_m, T_m, and ΔC_p contribute to the conformational stability (ΔG^{Aq}) of the protein.[16] As these thermodynamic parameters are related to the conformation and/or structure of the protein in folded and unfolded states, these values are often used to extract the structural information for the folded and unfolded states of the protein.

The temperature dependence of the free energy of unfolding, ΔG^{Aq}, for WT cyt c_{552} and its mutants (Figure 6) obtained from the analyses of the far-UV CD results at different denaturant concentrations were fit to the modified Gibbs−Helmholtz equation (eq 4). The values of the thermodynamic parameters obtained from the analyses of the data are listed in Table 1. The values of thermodynamic parameters such as ΔH_m and T_m for the unfolding of the secondary structure of the M69H mutant

dx.doi.org/10.1021/bi300982v | *Biochemistry* 2013, 52, 1373−1384

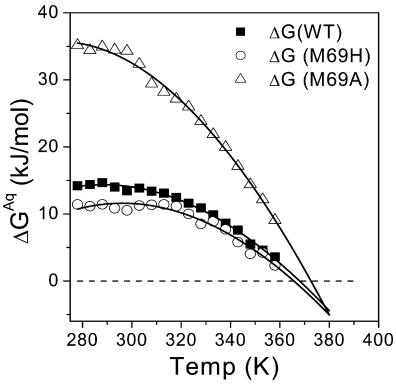

Figure 6. Protein stability curves plotted for the secondary structure of ferric WT (■), M69H (○), and M69A (△) cyt c_{552}. Each point in the stability curves represents the free energy of unfolding (ΔG^{Aq}) at the corresponding temperature. The solid lines represent nonlinear curve fits to the Gibbs–Helmholtz equation (eq 4).

were smaller than those of WT cyt c_{552} (Table 1), while the ΔC_p for the M69H mutant was within error of that of the WT protein. The stability curve for the M69A mutant was, on the other hand, found to be significantly higher than that of WT cyt c_{552} and that of the M69H mutant (Figure 6) possibly because of the higher ΔH_m of the M69A mutant.

Electrochemistry of WT and Mutant cyt c_{552}. The redox potential of iron in the heme is sensitive to the protein environment around the heme center; thus, the measurement of the redox potentials of the metal center in the protein can provide important redox state-dependent structural information about the folded and unfolded states of WT and mutant cyt c_{552}. The thermodynamics of the reduced form of the redox protein can be determined from the electrochemical studies of the folded and unfolded states (see below). Direct (unmediated) cyclic voltammetry (CV) and square wave voltammetry (SWV) of the folded and unfolded states of WT and mutant cyt c_{552} at the bare glassy carbon electrode were investigated to determine the effect of axial ligand mutation on the redox properties.

Midpoint Potential of Folded cyt c_{552}. Both the folded and unfolded forms of the WT and mutants (M69H and M69A) of cyt c_{552} show one-electron, quasi-reversible electrochemical behavior. The folded forms of WT, M69H, and M69A mutant cyt c_{552} exhibited redox potentials of 200, 40, and 130 mV versus the NHE, respectively, at pH 7.0 (Table 2 and Figures S6A and S7A of the Supporting Information). The redox potential of folded WT c_{552} (200 mV) agreed with that reported previously[24] and was also found to be well within the potential range of class I cyt *c* forms reported previously.[30]

The high positive redox potential for WT cyt c_{552} was assigned to the presence of a hydrophobic and strong π electron acceptor axial ligand, methionine.[30] It was suggested that the presence of methionine at the axial position of WT cyt c_{552} stabilizes the reduced state compared to its oxidized state.[30] In contrast, M69H (40 mV vs the NHE) showed a 160 mV lower redox potential compared to that of WT cyt c_{552}. Considering that the folded form of the M69H mutant consists of a bis-histidine coordination to the heme, the observed low redox potential for this mutant (M69H) was attributed to the polar, strong electron donating character of histidine, which prefers to form a strong bond with ferric iron and hence stabilizes the ferric state compared to the ferrous state. The bis-histidine species (M80H) of horse heart cyt *c* also showed a midpoint potential of 41 mV,[9] which is very similar to that of the M69H mutant in this study. The earlier report also showed that the redox potential decreases from 260 mV (vs the NHE) to 50 mV (vs the NHE) upon mutation of the axial methionine ligand with histidine (M61H) in cyt c_{551} from *Pseudomonas stutzeri*.[53] Axial coordination of imidazole in the heme peptide also earlier was shown to decrease the redox potential,[65] which agrees with the results presented here. The redox potential of M69A mutant cyt c_{552} was found to be 130 mV versus the NHE, indicating that the removal of the axial methionine indeed causes a decrease in the redox potential. The midpoint potential for the M80A mutant of horse heart cyt *c* was earlier shown to be 185 mV versus the NHE,[8] which is 75 mV lower than that of WT horse heart cyt *c*. This is consistent with the observed decrease in the redox potential of the M69A mutant with respect to WT cyt c_{552} in the case presented here.

Midpoint Potential of Unfolded cyt c_{552}. The redox potential of cyt c_{552} in the unfolded form provides insight into the ligand environment and the extent of solvent accessibility of the heme in the unfolded state. The results show that the redox potential of the heme of the WT and M69A mutant of cyt c_{552} decreased significantly upon unfolding, while that of the M69H mutant remains almost the same in the folded and unfolded forms of the protein (Table 2). Table 2 shows that the unfolded forms (in 7 M GdnHCl) of both WT and M69H mutant cyt c_{552} exhibit the same redox potential of 70 mV (vs the NHE). On the other hand under the same denaturing condition (in 7 M GdnHCl), the M69A mutant of cyt c_{552} exhibits a redox potential of −30 mV versus the NHE (Table 2 and Figures S6B and S7B of the Supporting Information).

As discussed in the previous section, the spectral features of the ferric forms of the WT and the M69H mutant are identical in the unfolded state (Figure 5), indicating that they possibly have similar environments around the heme in the oxidized forms of the metal ion. The observation of the same redox potential (Table 2) for the unfolded states of the WT and M69H mutant of cyt c_{552} suggests that the reduced forms of the unfolded WT and M69H mutant of cyt c_{552} are also possibly similar to each other. The predominant species in unfolded horse heart cyt *c* at pH 7.4 was shown to be bis-histidine coordinated to the heme, having a redox potential of −200 mV versus the NHE.[66] The redox potential of the unfolded WT and M69H mutant of cyt c_{552} (70 mV) at neutral pH was not only higher than that of unfolded horse heart cyt *c* (−200 mV) but also higher than that of the folded M69H (40 mV) mutant of cyt c_{552} (Table 2). This result thus indicates that unlike

Table 2. Midpoint Potentials ($E°'$) Obtained by Cyclic Voltammetry for the Folded and Unfolded States of WT cyt c_{552} and Its Axial Ligand Variant Proteins from *T. thermophilus* at pH 7.0 and 25 °C[a]

protein	$E_F°'$ (mV vs NHE)	$E_U°'$ (mV vs NHE)	ΔG^{Aq}_{Red} (kJ/mol)
WT	200 ± 7 (198 ± 5)	70 ± 8 (65 ± 10)	26 ± 2
M69H	40 ± 8 (55 ± 13)	70 ± 7 (73 ± 8)	7 ± 2
M69A	130 ± 10 (125 ± 10)	−30 ± 7 (−25 ± 8)	49 ± 2

[a]The value in parentheses corresponds to the midpoint potential obtained via square wave voltammetry. The ΔG^{Aq}_{Red} values for the reduced proteins were calculated by using the relation in Scheme 1.

dx.doi.org/10.1021/bi300982v | *Biochemistry* 2013, 52, 1373−1384

unfolded horse heart cyt *c*, the unfolded WT and the unfolded M69H mutant of cyt c_{552} possibly do not possess the His/His coordination of the heme. This observation suggests that the predominant species in unfolded WT cyt c_{552} and the M69H mutant protein might consist of the heme with axial coordination of His and H_2O.

The redox potential of the unfolded M69A mutant at neutral pH was found to be negative (−30 mV) compared to those of the unfolded WT and the unfolded M69H (70 mV) mutant of cyt c_{552}. The redox potential (−30 mV) for the unfolded M69A mutant of cyt c_{552} was higher than that reported for the misfolded bis-histidine heme species in unfolded horse heart cyt *c* (−200 mV). This result supports the idea that the unfolded M69A mutant of cyt c_{552} may consist of an axial ligand from the protein matrix as proposed in the previous section.

Conformational Stability of Reduced cyt c_{552}. A thermodynamic cycle can be constructed connecting the oxidized and reduced states of cyt c_{552} in its folded and unfolded configurations as shown in Scheme 1. The conformational stability [ΔG^{Aq}_{Ox} (see Table 1 for the ΔG^{Aq} of the oxidized protein)] of the oxidized state of WT and mutant cyt c_{552} and their respective redox potentials in both folded and unfolded states were available from the direct electrochemistry and unfolding studies. Thus, the conformational stabilities (ΔG^{Aq}_{Red}) of these species in their reduced state were determined (Table 2) by using the scheme with the help of the following equation (eq 5):

$$\Delta G^{Aq}_{Red} = \Delta G^{Aq}_{Ox} - F(E_U{}^{\circ\prime} - E_F{}^{\circ\prime}) \quad (5)$$

where *F* is the Faraday constant (96485 J/V) and $E_U{}^{\circ\prime}$ and $E_F{}^{\circ\prime}$ are the standard redox potentials for the unfolded and folded forms of the protein (in volts), respectively.

The results (Tables 1 and 2) from the analyses described above suggest that the conformational stabilities (ΔG^{Aq}_{Red}) of WT and M69A cyt c_{552} in their reduced states are higher than those of their respective oxidized states. As discussed earlier, Met69 forms a stronger bond with the ferrous (due to soft−soft interaction) form of iron than with the ferric form (soft−hard interaction) of cyt c_{552}[67] and hence provides a higher conformational stability to the WT species in its reduced state. These results agree with the earlier study on the effects of the axial coordination in the ferric and in ferrous forms of the heme octapeptide derived from cyt *c*.[67] On the other hand, the conformational stability of M69H cyt c_{552} in the reduced state [ΔG^{Aq}_{Red} = 7 ± 2 kJ/mol (Table 2)] is only slightly lower than that of the corresponding oxidized state [ΔG^{Aq}_{Ox} = 10 ± 2 kJ/mol (Table 1)], indicating that the oxidation state of the metal ion may not have any significant effect on the conformational stability of the M69H mutant of cyt c_{552} (Tables 1 and 2).

Scheme 1. Thermodynamic Cycle That Connects the Four States (oxidized and reduced, folded and unfolded) of WT and Mutant cyt c_{552}[a]

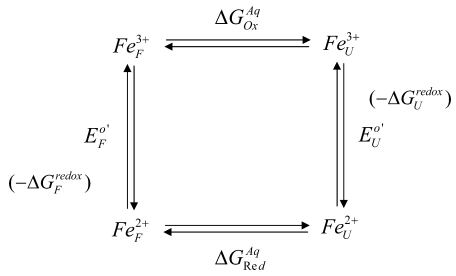

[a] ΔG^{Aq} values for the reduced proteins were calculated by using the relation $\Delta G^{Aq}_{Red} = \Delta G^{Aq}_{Ox} + F(E_F{}^{\circ\prime} - E_U{}^{\circ\prime})$. U, F, Ox, and Red represent unfolded, folded, oxidized, and reduced states of the protein, respectively.

CONCLUSIONS

The replacement of Met69 with His or Ala affected the heme tertiary structure but had almost no effect on the secondary structure of mutant cyt c_{552}. The redox potential of the heme was lowered by both the M69H and M69A mutations. The lower conformational stability (ΔG^{Aq}_S) of the M69H mutant protein compared to that of WT cyt c_{552} may be ascribed to the lower enthalpy of unfolding at the T_m (ΔH_m) in the mutant protein. The lower enthalpy of unfolding of the M69H mutant compared to that of WT cyt c_{552} might result from the introduction of the polar histidine residue in place of the hydrophobic methionine residue inside the compact hydrophobic heme pocket of the protein. The higher thermal and conformational stabilities of the M69A mutant versus those of WT and M69H cyt c_{552} were attributed to the increased ΔH_m. The spectroscopic results indicated that the conformations of the heme (i.e., coordination geometry and environment) in the unfolded state for both the WT and the M69H mutant of the protein were similar to each other, with a high-spin ferric heme in an isotropic environment. The M69A mutant, on the other hand, showed a distinctly different unfolded structure with a low-spin character of the heme active site. The unfolded state was proposed to consist of His/H_2O ligation of the heme in the WT and the M69H mutant, while that in case of the unfolded M69A mutant was either His/His or His/N_{ter} NH_2 or His/O ligation to the heme. The conformational stabilities (ΔG^{Aq}_{Red}) of WT and M69A cyt c_{552} in their reduced states were higher than those in their respective oxidized states, while both oxidized and reduced states have similar conformational stabilities in the case of the M69H mutant of cyt c_{552}. The results thus suggest that although the axial methionine in thermostable cyt c_{552} is crucial for the electron transport function of the protein, removal of the axial coordination could enhance the apparent conformational stability and thermostability of the protein.

ASSOCIATED CONTENT

Supporting Information

Crystal structure (PDB entry 1C52) of thermostable cyt c_{552} illustrating the compact hydrophobic environment around the distal heme pocket, ^{1}H NMR spectra of the oxidized protein and its mutant, tryptophan fluorescence spectra, GdnHCl-dependent UV−visible absorption spectra, temperature-dependent Soret and visible absorption spectra of the ferric M69A mutant, GdnHCl-dependent heme CD spectra of the ferric forms of the mutants, cyclic voltammograms of the WT and mutants of cyt c_{552} in their native and denatured states, square wave voltammograms of the WT and mutants of cyt c_{552} in their native and denatured states, comparison of the sequences of different forms of cyt *c* with that of cyt c_{552}, analyses of far-UV CD spectra of the proteins by Reed's method, and UV−visible absorption spectral features for both ferric and ferrous states of WT and mutant cyt c_{552} and some similar heme proteins. This material is available free of charge via the Internet at http://pubs.acs.org.

AUTHOR INFORMATION

Corresponding Author

*S.M.: e-mail, shyamal@tifr.res.in. R.K.B.: e-mail, rkbchemistry@gmail.com; telephone, 009122 22782363; fax, 009122 2280 4610.

Present Address

[‖]Children's Hospital Oakland Research Institute (CHORI), 5700 Martin Luther King Jr. Way, Oakland, CA 94609.

Funding

This work was supported by the Tata Institute of Fundamental Research (Mumbai, India), the 21st Century COE Programme, Japan, and the Department of Science and Technology (New Delhi, India). A part of this work was supported by Grant-in-Aid for Scientific Research (No. 24225004) from the Ministry of Education, Culture, Sports, Science and Technology (MEXT), Japan.

Notes

The authors declare no competing financial interest.

ACKNOWLEDGMENTS

We thank Mr. B. T. Kansara for help in conducting the experiments and Dr. Soumen Kanti Manna for suggestions and discussions.

DEDICATION

Dedicated to the memory of Prof. Ivano Bertini.

ABBREVIATIONS

cyt *c*, cytochrome *c*; WT, wild type; M69H and M69A, methionine 69 to histidine and alanine mutants of cyt c_{552}, respectively; CD, circular dichroism; GdnHCl, guanidine hydrochloride; T_m, midpoint unfolding (melting) temperature; C_m, midpoint of unfolding concentration of denaturant, e.g., $[GdnHCl]_{1/2}$; ΔG_U, free energy of unfolding; ΔG_U^{Aq}, free energy of unfolding in an aqueous solvent; ΔH_m, enthalpy of unfolding at the T_m; ΔS_m, entropy of unfolding at the T_m; ΔC_p, heat capacity of unfolding; CV, cyclic voltammetry; SWV, square wave voltammetry; $E_F^{\circ\prime}$, midpoint potential of the folded protein; $E_U^{\circ\prime}$, midpoint potential of the unfolded protein; 1C52, PDB entry for cyt c_{552} from *T. thermophilus*; 1YCC, PDB entry for yeast iso-1-cytochrome *c*; 1HRC, PDB entry for horse cyt *c*; 1YNR, PDB entry for cyt c_{552} (*Ht* cyt c_{552}) from *H. thermophilus*.

REFERENCES

(1) Sono, M., Roach, M. P., Coulter, E. D., and Dawson, J. H. (1996) Heme-Containing Oxygenases. *Chem. Rev. 96*, 2841−2888.

(2) Bertini, I., Gray, H. B., Lippard, S. J., and Valentine, J. S. (1994) *Bioinorganic Chemistry*, University Science Books, Sausalito, CA.

(3) Poulos, T. L. (1996) The role of the proximal ligand in heme enzymes. *J. Biol. Inorg. Chem. 1*, 356−359.

(4) McLendon, G., and Sandberg, K. (1978) Axial ligand effects on myoglobin stability. *J. Biol. Chem. 253*, 3913−3917.

(5) Hamada, D., Kuroda, Y., Kataoka, M., Aimoto, S., Yoshimura, T., and Goto, Y. (1996) Role of heme axial ligands in the conformational stability of the native and molten globule states of horse cytochrome c. *J. Mol. Biol. 256*, 172−186.

(6) Satoh, T., Itoga, A., Isogai, Y., Kurihara, M., Yamada, S., Natori, M., Suzuki, N., Suruga, K., Kawachi, R., Arahira, M., Nishio, T., Fukazawa, C., and Oku, T. (2002) Increasing the conformational stability by replacement of heme axial ligand in c-type cytochrome. *FEBS Lett. 531*, 543−547.

(7) Kamiya, N., Okimoto, Y., Ding, Z., Ohtomo, H., Shimizu, M., Kitayama, A., Morii, H., and Nagamune, T. (2001) How does heme axial ligand deletion affect the structure and the function of cytochrome b_{562}? *Protein Eng. 14*, 415−419.

(8) Wallace, C. J., and Clark-Lewis, I. (1992) Functional role of heme ligation in cytochrome c. Effects of replacement of methionine 80 with natural and non-natural residues by semisynthesis. *J. Biol. Chem. 267*, 3852−3861.

(9) Raphael, A. L., and Gray, H. B. (1989) Axial ligand replacement in horse heart cytochrome c by semisynthesis. *Proteins 6*, 338−340.

(10) Sligar, S. G., and Egeberg, K. D. (1987) Alteration of Heme Axial Ligands by Site-Directed Mutagenesis: A Cytochrome Becomes a Catalytic Demethylase. *J. Am. Chem. Soc. 109*, 7896−7897.

(11) Louro, R. O., de Waal, E. C., Ubbink, M., and Turner, D. L. (2002) Replacement of the methionine axial ligand in cytochrome c_{550} by a lysine: Effects on the haem electronic structure. *FEBS Lett. 510*, 185−188.

(12) Behera, R. K., Goyal, S., and Mazumdar, S. (2010) Modification of the heme active site to increase the peroxidase activity of thermophilic cytochrome P450: A rational approach. *J. Inorg. Biochem. 104*, 1185−1194.

(13) Pace, C. N., Shirley, B. A., McNutt, M., and Gajiwala, K. (1996) Forces contributing to the conformational stability of proteins. *FASEB J. 10*, 75−83.

(14) Robertson, A. D., and Murphy, K. P. (1997) Protein Structure and the Energetics of Protein Stability. *Chem. Rev. 97*, 1251−1268.

(15) Luckey, M., Ling, R., Dose, A., and Malloy, B. (1991) Role of a disulfide bond in the thermal stability of the LamB protein trimer in *Escherichia coli* outer membrane. *J. Biol. Chem. 266*, 1866−1871.

(16) Razvi, A., and Scholtz, J. M. (2006) Lessons in stability from thermophilic proteins. *Protein Sci. 15*, 1569−1578.

(17) Vogt, G., Woell, S., and Argos, P. (1997) Protein thermal stability, hydrogen bonds, and ion pairs. *J. Mol. Biol. 269*, 631−643.

(18) Beadle, B. M., Baase, W. A., Wilson, D. B., Gilkes, N. R., and Shoichet, B. K. (1999) Comparing the thermodynamic stabilities of a related thermophilic and mesophilic enzyme. *Biochemistry 38*, 2570−2576.

(19) Behera, R. K., and Mazumdar, S. (2010) Thermodynamic basis of the thermostability of CYP175A1 from *Thermus thermophilus*. *Int. J. Biol. Macromol. 46*, 412−418.

(20) Vogt, G., and Argos, P. (1997) Protein thermal stability: Hydrogen bonds or internal packing? *Folding Des. 2*, S40−S46.

(21) Stepanenko, O. V., Marabotti, A., Kuznetsova, I. M., Turoverov, K. K., Fini, C., Varriale, A., Staiano, M., Rossi, M., and D'Auria, S. (2008) Hydrophobic interactions and ionic networks play an important role in thermal stability and denaturation mechanism of the porcine odorant-binding protein. *Proteins 71*, 35−44.

(22) Bren, K. L., and Gray, H. B. (1993) Structurally Engineered Cytochromes with Novel Ligand-Binding Sites: Oxy and Carbon Monoxy Derivatives of Semisynthetic Horse Heart Ala80 Cytochrome c. *J. Am. Chem. Soc. 115*, 10382−10383.

(23) Nakajima, H., Ichikawa, Y., Satake, Y., Takatani, N., Manna, S. K., Rajbongshi, J., Mazumdar, S., and Watanabe, Y. (2008) Engineering of *Thermus thermophilus* cytochrome c552: Thermally tolerant artificial peroxidase. *ChemBioChem 9*, 2954−2957.

(24) Fee, J. A., Chen, Y., Todaro, T. R., Bren, K. L., Patel, K. M., Hill, M. G., Gomez-Moran, E., Loehr, T. M., Ai, J., Thony-Meyer, L., Williams, P. A., Stura, E., Sridhar, V., and McRee, D. E. (2000) Integrity of *Thermus thermophilus* cytochrome c552 synthesized by *Escherichia coli* cells expressing the host-specific cytochrome c maturation genes, ccmABCDEFGH: Biochemical, spectral, and structural characterization of the recombinant protein. *Protein Sci. 9*, 2074−2084.

(25) Than, M. E., Hof, P., Huber, R., Bourenkov, G. P., Bartunik, H. D., Buse, G., and Soulimane, T. (1997) *Thermus thermophilus* cytochrome-c552: A new highly thermostable cytochrome-c structure obtained by MAD phasing. *J. Mol. Biol. 271*, 629−644.

(26) Berry, E. A., and Trumpower, B. L. (1987) Simultaneous determination of hemes a, b, and c from pyridine hemochrome spectra. *Anal. Biochem. 161*, 1−15.
(27) Ferreon, A. C., and Bolen, D. W. (2004) Thermodynamics of denaturant-induced unfolding of a protein that exhibits variable two-state denaturation. *Biochemistry 43*, 13357−13369.
(28) Pace, C. N., and Shaw, K. L. (2000) Linear extrapolation method of analyzing solvent denaturation curves. *Proteins 4* (Suppl.), 1−7.
(29) Fersht, A. (1999) *Structure and Mechanism in Protein Science: A Guide to Enzyme Catalysis and Protein Folding*, W. H. Freeman and Co., New York.
(30) Moore, G. R., and Pettigrew, G. W. (1990) *Cytochromes c: Evolutionary, Structural and Physiochemical Aspects*, Springer-Verlag, Berlin.
(31) Behera, R. K., and Mazumdar, S. (2008) Roles of two surface residues near the access channel in the substrate recognition by cytochrome P450cam. *Biophys. Chem. 135*, 1−6.
(32) Roach, M. P., Puspita, W. J., and Watanabe, Y. (2000) Proximal ligand control of heme iron coordination structure and reactivity with hydrogen peroxide: Investigations of the myoglobin cavity mutant H93G with unnatural oxygen donor proximal ligands. *J. Inorg. Biochem. 81*, 173−182.
(33) Adak, S., Mazumdar, A., and Banerjee, R. K. (1997) Low catalytic turnover of horseradish peroxidase in thiocyanate oxidation. Evidence for concurrent inactivation by cyanide generated through one-electron oxidation of thiocyanate. *J. Biol. Chem. 272*, 11049−11056.
(34) Ichikawa, Y., Nakajima, H., and Watanabe, Y. (2006) Characterization of peroxide-bound heme species generated in the reaction of thermally tolerant cytochrome c552 with hydrogen peroxide. *ChemBioChem 7*, 1582−1589.
(35) Russell, B. S., Melenkivitz, R., and Bren, K. L. (2000) NMR investigation of ferricytochrome c unfolding: Detection of an equilibrium unfolding intermediate and residual structure in the denatured state. *Proc. Natl. Acad. Sci. U.S.A. 97*, 8312−8317.
(36) Walker, F. A., Ed. (2000) *Proton NMR and EPR Spectroscopy of Paramagnetic Metalloporphyrins*, Vol. *5*, Academic Press, New York.
(37) Bertini, I., Turano, P., and Vila, A. J. (1993) Nuclear magnetic resonance of paramagnetic metalloproteins. *Chem. Rev. 93*, 2833−2932.
(38) LaMar, G. N., Satterlee, J. D., and DeRopp, J. S. (2000) Nuclear magnetic resonance of hemeproteins. In *The Porphyrin Handbook* (Kadish, K. M., Smith, K. M., and Guilard, R., Eds.) pp 185−298, Academic Press, San Diego.
(39) Kelly, S. M., Jess, T. J., and Price, N. C. (2005) How to study proteins by circular dichroism. *Biochim. Biophys. Acta 1751*, 119−139.
(40) Reed, J., and Reed, T. A. (1997) A Set of Constructed Type Spectra for the Practical Estimation of Peptide Secondary Structure from Circular Dichroism. *Anal. Biochem. 254*, 36−40.
(41) Chattopadhyay, K., and Mazumdar, S. (2003) Stabilization of partially folded states of cytochrome c in aqueous surfactant: Effects of ionic and hydrophobic interactions. *Biochemistry 42*, 14606−14613.
(42) Hsu, M. C., and Woody, R. W. (1971) The origin of the heme Cotton effects in myoglobin and hemoglobin. *J. Am. Chem. Soc. 93*, 3515−3525.
(43) Wittung-Stafshede, P. (1998) A stable, molten-globule-like cytochrome c. *Biochim. Biophys. Acta 1382*, 324−332.
(44) Travaglini-Allocatelli, C., Gianni, S., Morea, V., Tramontano, A., Soulimane, T., and Brunori, M. (2003) Exploring the Cytochrome c Folding Mechanism. *J. Biol. Chem. 278*, 41136−41140.
(45) Tai, H., Kawano, S., and Yamamoto, Y. (2008) Characterization of N-terminal amino group-heme ligation emerging upon guanidine hydrochloric acid induced unfolding of *Hydrogenobacter thermophilus* ferricytochrome c_{552}. *J. Biol. Inorg. Chem. 13*, 25−34.
(46) Fedurco, M., Augustynski, J., Indiani, C., Smulevich, G., Antalik, M., Bano, M., Sedlak, E., Glascock, M. C., and Dawson, J. H. (2004) The heme iron coordination of unfolded ferric and ferrous cytochrome c in neutral and acidic urea solutions. Spectroscopic and electrochemical studies. *Biochim. Biophys. Acta 1703*, 31−41.
(47) Russell, B. S., and Bren, K. L. (2002) Denaturant dependence of equilibrium unfolding intermediates and denatured state structure of horse ferricytochrome c. *J. Biol. Inorg. Chem. 7*, 909−916.
(48) Travaglini-Allocatelli, C., Gianni, S., Dubey, V. K., Borgia, A., Di Matteo, A., Bonivento, D., Cutruzzolà, F., Bren, K. L., and Brunori, M. (2005) An Obligatory Intermediate in the Folding Pathway of Cytochrome c552 from *Hydrogenobacter thermophilus*. *J. Biol. Chem. 280*, 25729−25734.
(49) Bartalesi, I., Bertini, I., Di Rocco, G., Ranieri, A., Rosato, A., Vanarotti, M., Vasos, P. R., and Viezzoli, M. S. (2004) Protein stability and mutations in the axial methionine loop of a minimal cytochrome c. *J. Biol. Inorg. Chem. 9*, 600−608.
(50) Zhong, L., Wen, X., Rabinowitz, T. M., Russell, B. S., Karan, E. F., and Bren, K. L. (2004) Heme axial methionine fluxionality in *Hydrogenobacter thermophilus* cytochrome c552. *Proc. Natl. Acad. Sci. U.S.A. 101*, 8637−8642.
(51) Wen, X., Patel, K. M., Russell, B. S., and Bren, K. L. (2007) Effects of heme pocket structure and mobility on cytochrome c stability. *Biochemistry 46*, 2537−2544.
(52) Yamamoto, Y., Terui, N., Tachiiri, N., Minakawa, K., Matsuo, H., Kameda, T., Hasegawa, J., Sambongi, Y., Uchiyama, S., Kobayashi, Y., and Igarashi, Y. (2002) Influence of amino acid side chain packing on Fe-methionine coordination in thermostable cytochrome c. *J. Am. Chem. Soc. 124*, 11574−11575.
(53) Miller, G. T., Zhang, B., Hardman, J. K., and Timkovich, R. (2000) Converting a c-type to a b-type cytochrome: Met61 to His61 mutant of *Pseudomonas* cytochrome c-551. *Biochemistry 39*, 9010−9017.
(54) Dolla, A., Florens, L., Bruschi, M., Dudich, I. V., and Makarov, A. A. (1995) Drastic influence of a single heme axial ligand replacement on the thermostability of cytochrome c3. *Biochem. Biophys. Res. Commun. 211*, 742−747.
(55) Lu, Y., Casimiro, D. R., Bren, K. L., Richards, J. H., and Gray, H. B. (1993) Structurally engineered cytochromes with unusual ligand-binding properties: Expression of *Saccharomyces cerevisiae* Met-80→Ala iso-1-cytochrome c. *Proc. Natl. Acad. Sci. U.S.A. 90*, 11456−11459.
(56) Sosnick, T. R., Mayne, L., Hiller, R., and Englander, S. W. (1994) The barriers in protein folding. *Nat. Struct. Biol. 1*, 149−156.
(57) Elove, G. A., Bhuyan, A. K., and Roder, H. (1994) Kinetic mechanism of cytochrome c folding: Involvement of the heme and its ligands. *Biochemistry 33*, 6925−6935.
(58) Colon, W., Wakem, L. P., Sherman, F., and Roder, H. (1997) Identification of the predominant non-native histidine ligand in unfolded cytochrome c. *Biochemistry 36*, 12535−12541.
(59) Hayashi, Y., Nagao, S., Osuka, H., Komori, H., Higuchi, Y., and Hirota, S. (2012) Domain Swapping of the Heme and N-Terminal α-Helix in *Hydrogenobacter thermophilus* Cytochrome c_{552} Dimer. *Biochemistry 51*, 8608−8616.
(60) Hirota, S., Hattori, Y., Nagao, S., Taketa, M., Komori, H., Kamikubo, H., Wang, Z., Takahashi, I., Negi, S., Sugiura, Y., Kataoka, M., and Higuchi, Y. (2010) Cytochrome c polymerization by successive domain swapping at the C-terminal helix. *Proc. Natl. Acad. Sci. U.S.A. 107*, 12854−12859.
(61) Shortle, D. (1996) The denatured state (the other half of the folding equation) and its role in protein stability. *FASEB J. 10*, 27−34.
(62) Dill, K. A., and Shortle, D. (1991) Denatured states of proteins. *Annu. Rev. Biochem. 60*, 795−825.
(63) Robic, S., Guzman-Casado, M., Sanchez-Ruiz, J. M., and Marqusee, S. (2003) Role of residual structure in the unfolded state of a thermophilic protein. *Proc. Natl. Acad. Sci. U.S.A. 100*, 11345−11349.
(64) Becktel, W. J., and Schellman, J. A. (1987) Protein stability curves. *Biopolymers 26*, 1859−1877.
(65) Chattopadhyay, K., and Mazumdar, S. (1997) Direct electrochemistry of heme undecapeptide in aqueous surfactant solutions: The effect of hydrophobicity and axial ligation on redox potential of heme. *Curr. Sci. 73*, 65−68.

(66) Fedurco, M., Augustynski, J., Indiani, C., Smulevich, G., Antalik, M., Bano, M., Sedlak, E., Glascock, M. C., and Dawson, J. H. (2005) Electrochemistry of unfolded cytochrome c in neutral and acidic urea solutions. *J. Am. Chem. Soc. 127*, 7638−7646.
(67) Tezcan, F. A., Winkler, J. R., and Gray, H. B. (1998) Effects of Ligation and Folding on Reduction Potentials of Heme Proteins. *J. Am. Chem. Soc. 120*, 13383−13388.